The first external loop of the metal ion transporter DCT1 is involved in metal ion binding and specificity

Adiel Cohen*, Yaniv Nevo*, and Nathan Nelson†

Department of Biochemistry, The George S. Wise Faculty of Life Sciences, Tel Aviv University, Tel Aviv 69978, Israel

Communicated by H. Ronald Kaback, University of California, Los Angeles, CA, July 21, 2003 (received for review March 11, 2003)

The yeast null mutant *smf1*Δ cannot grow on medium containing EGTA. Expression of Smf1p or the mammalian transporter DCT1 (Slc11a2) suppresses the above-mentioned phenotype. Both can also be expressed in *Xenopus* oocytes, and the uptake activity and their electrophysiological properties can be studied. We used these systems to analyze the properties of mutations in the predicted external loop I of DCT1. The sensitivity of the transporter to amino acid substitutions in this region is manifested by the mutation G119A, which resulted in almost complete inhibition of the metal ion uptake activity and marked changes in the pre-steady-state currents in *Xenopus* oocytes. The mutation Q126D abolished the uptake and the electrophysiology, but the double mutant D124A/Q126D partially restored it and changed the metal ion specificity in favor of Fe^{2+}. The maximal pre-steady-state currents at negatively imposed potentials shifted to a lower pH of ≈5. The triple mutant G119A/D124A/Q126D, which has no apparent transport activity, exhibited remarkable pre-steady-state currents at pH 7.5. Moreover, Zn^{2+} had a dual effect on this mutant; at pH 7.5 it eliminated the pre-steady state without generating steady-state currents, and at pH 5.5 it induced large pre-steady-state currents. The mutant D124A retained appreciable Fe^{2+} uptake activity but exhibited very little Mn^{2+} uptake at pH 5.5 and was abolished at pH 6.5. The properties of the various mutants suggest that loop I is involved in the metal ion binding and its coupling to the proton-driving force.

mutations | uptake | electrophysiology | yeast | oocytes

In the last few years it has become apparent that, from bacteria to man, the family of natural resistance-associated macrophage protein (NRAMP) metal ion transporters plays a major role in metal ion homeostasis (1–4). This family is represented in yeast by three genes (*SMF1*, *SMF2*, and *SMF3*) and in mammals by NRAMP1 and NRAMP2 (DCT1). The family members function as general metal ion transporters and can transport not only Mn^{2+} and Cu^{2+} (5) but also Fe^{2+}, Cd^{2+}, Ni^{2+}, and Co^{2+} (6–8). Expression of DCT1 and Smf1p in *Xenopus* oocytes demonstrated that the driving force for the divalent metal ion transport is H^+-dependent (8, 9). In addition, in the expressing oocytes, a large H^+ slip through DCT1 and Na^+ slippage through Smf1p was observed (8, 10). The identity of the substrate and proton-binding sites on the transporters are not known, and the mechanism of metal ion transport is obscure. Few conserved amino acids were changed in Smf1p (11) and DCT1 (12, 13), but the results have not yet revealed many aspects of the action mechanism of these transporters. We developed a concerted approach for the study of Smf1p and DCT1. It uses yeast null mutants lacking the SMF metal ion transporters (14), and *Xenopus* oocytes, where those transporters are absent, as an expression medium for Smf1p and DCT1 in appropriate plasmids (10). The null mutant *smf1*Δ is unable to grow in the presence of EGTA (5, 14). Expression of Smf1p or the mammalian transporter DCT1 suppresses the above-mentioned phenotype and allows growth of the yeast mutant in the presence of EGTA. In yeast, inactive mutations in Smf1p or DCT1 could be rescued by spontaneous or random mutagenesis (12, 15). Expression of the same genes in parallel in *Xenopus* oocytes are ideal heterologous expression systems for metal ion transporters (16), which can reveal retained partial activities of the transporter that we are unable to measure in the yeast system.

Materials and Methods

Yeast Strains and Site-Directed Mutagenesis of DCT1. The "wild type" used was *Saccharomyces cerevisiae* W303 (*MATa*/α *trp1 ade2 his3 leu2 ura3*). The other strain was *smf1*Δ (*MATa ade2 his3 leu2 ura3 SMF1*::*URA3*). Yeast were grown and transformation was performed as described (14, 15, 17). Oligonucleotide-directed, site-specific mutagenesis was performed by overlapping nucleotides with the mutation by using the PCR method (15). The DCT1 gene cloned into BFG plasmid (BFG-DCT1) was used as a template for PCR mutagenesis. *Nde*I and *Spe*I restriction sites were introduced at positions 145 and 1,719 of the DCT1 reading frame. This resulted in the substitutions G50M, S573T, and V574S, which did not change the properties of DCT1. All the mutations were confirmed by sequence analysis. The transformation of the *smf1*Δ null mutants was performed by following published procedures (14).

Oocyte Preparation and Uptake Measurements. *Xenopus laevis* oocytes were handled as described (10). Uptake experiments were performed 3–7 days after injections. Uptake solution for radiotracer experiments contained 100 mM NaCl or choline chloride/10 mM Hepes/2 mM Mes/2 mM KCl/1 mM $CaCl_2$/1 mM $MgCl_2$/2 mM L-ascorbic acid (where indicated), and the pH was adjusted to 5.5–7.5 with Tris base. Usually 15 oocytes were incubated in 0.5 ml of a solution containing $^{55}FeCl_2$, $^{54}MnCl_2$, $^{65}ZnCl^{+2}$, or $^{60}CoCl_2$. The radioactive tracer was usually mixed with 2–20 μM unlabeled metal ion, and the uptake was followed for 20–30 min. The numbers given in *Results* are background-corrected and expressed in specific activity (pmol per oocyte per h). Specific activity of <0.1 is not significant under our experimental conditions.

Electrophysiological Experiments. Experiments with the two-microelectrode voltage-clamp technique were performed as described (18–20). Data analysis was performed as described (10). To analyze the pre-steady-state currents, the current traces were fitted to $I(t) = I_1 \exp(-t/\tau_1) + I_2 \exp(-t/\tau_2) + I_{ss}$, where I_1 is a capacitative current with time constant τ_1 associated with the oocyte plasma membrane (τ_1 is also observed in noninjected control oocytes), I_2 is a transient current associated with DCT1 expression with time constant τ_2, and I_{ss} is the steady-state current. The parameters τ_1, τ_2, I_1, I_2, and I_{ss} were allowed to vary in all fits. The transient charge movements Q were obtained from the time integrals of $I_{transient}(t) = I_2 \exp(-t/\tau_2)$ during the "on" and "off" responses for all depolarizing and hyperpolarizing potentials and fitted by the Boltzmann equation, $Q = Q_{max}/\{1 + \exp[(V - V_{0.5})zF/RT]\} + Q_{hyp}$, where Q_{max} represents the total charge movement, z represents the effective valence, $V_{0.5}$

Abbreviation: NRAMP, natural resistance-associated macrophage protein.

*A.C. and Y.N. contributed equally to this work.

†To whom correspondence should be addressed. E-mail: nelson@post.tau.ac.il.

www.pnas.org/cgi/doi/10.1073/pnas.1934572100

```
                          ****       *       **
Smf3p              16     DPGNYATSVSGGAQYKYTLL
Smf2p              66     DPGNYSTAVAAGSAHRYKLL
Smf1p              91     DPGNYSTAVDAGASNQFSLL
NRAMP1             86     DPGNIESDLQSGAVAGFKLL
NRAMP2 (DCT1)     117     DPGNIESDLQSGAVAGFKLL
Malvolio           93     DPGNIESDMQSGAAAKYKIL
AtNramp2           84     DPGNMETDLQAGAIAGYSLL
Mt MntH            49     DPGNVAANVSSGAQFGYLLL
MntH               34     DPGNFATNIQAGASFGYQLL
```

Fig. 1. Alignment of the putative external loop I of metal ion transporters of the NRAMP family in different species. The amino acid sequences were obtained from published papers and GenBank: the yeast Smf1p, Smf2p, and Smf3p are from refs. 5 and 14; the mouse NRAMP1 and rat NRAMP2 are from ref. 9; *Drosophila melanogaster* Malvolio is from GenBank accession no. P49283; *Arabidopsis thaliana* AtNramp2 is from GenBank accession no. AAD41078; *Mycobacterium tuberculosis* Mt MntH is from GenBank accession no. AAK45198; and *Escherichia coli* MntH is from GenBank accession no. NP311298.

represents the midpoint of the charge distribution, Q_{hyp} represents the charge movement for extreme hyperpolarizing potentials (18, 21), and R, T, and F are the usual thermodynamic constants.

Results

Usually, when homologous genes from a different origin complement the same null mutant in yeast, we assume that the nonconserved amino acids in both proteins are probably of minor importance. Consequently, it is a common practice to mutate the conserved amino acids in those proteins. We set out to check an opposite approach by substituting the nonconserved putative loop I of DCT1 with the first *SMF1* loop (see Fig. 1 for sequence alignment), but this substitution rendered the transporter completely inactive. We then switched only a part of this loop, the five residues ESDLQ with the corresponding sequence STAVD of Smf1p, and the activity of the resulting DCT1 mutant was also abolished (data not shown). This result indicated that the nonconserved amino acid residues of the first loop are of importance for the proper function of the transporter.

Mutations in Loop I of DCT1 According to the Amino Acid Sequence of Smf1p. The alignment of amino acid sequences of the predicted external loop I of the Nramp family is shown in Fig. 1. The sequence DPGN at the end of the first transmembrane segment is conserved in all of the family members, and the LL at the beginning of the second transmembrane segment is conserved in most of them. Except for a glycine residue (G128 in DCT1), all the other amino acids are not strictly conserved and the predicted external loop I has no apparent motifs (Fig. 1). It therefore was somewhat surprising that amino acid substitutions in this region resulted in drastic changes in the properties of the mutated transporter. Table 1 lists the DCT1 mutations that were generated, their uptake activity in *Xenopus* oocytes, and their ability to suppress the growth arrest in yeast mutants lacking the SMF1 gene (*Smf1*Δ). The data are of a representative experiment of at least three experiments with oocytes from different frogs. All the listed mutations resulted in decreased uptake activity of metal ions into the oocytes and in some to total inhibition of the uptake. Approximately 10% manganese uptake activity was sufficient for complementation of the yeast null *SMF1* mutant. Only the DCT1 mutations E122A (E122 was mutated to A instead of S because of the adjacent serine) and K134S retained the capability to suppress the growth arrest of *Smf1*Δ in yeast extract/peptone/dextrose medium containing EGTA. The mutation D124A exhibited Fe^{+2} uptake into *Xenopus* oocytes equivalent to that of the K134S mutant, yet it was inactive in suppressing the growth arrest of *Smf1*Δ on medium containing EGTA. Because it was shown previously that the growth arrest of the yeast mutant is due to the Mn^{+2} depletion in the medium (5), the very low Mn^{+2} uptake by the D124A mutant was probably not sufficient to complement the yeast phenotype.

The *SMF1* mutations S97E and S109K, which are the reciprocal mutations of E122A (see above about A substitution for S) and K134S, respectively, in DCT1, rendered a protein complementary to the yeast null mutant and enabled its growth on EGTA-containing plates. This means that both proteins are less sensitive to amino acid substitutions at these positions. The D101Q mutation in Smf1p and its reciprocal substitution of Q126D in DCT1 are both completely inactive in the yeast mutant complementation assay, which shows high sensitivity at this site. In the A99D mutation in Smf1p (reciprocal of D124A), a somewhat differential effect was observed because the mutated Smf1p complements the growth on pH 7.5 (only) of the yeast triple mutant (14), whereas the parallel D124A mutation of DCT1 was completely inactive in this complementation assay. Here the DCT1 is more sensitive than Smf1p to the reciprocal mutation.

Metal Ion Specificity of the DCT1 Mutants. The metal ion specificity toward the different metal ions changed in some of the mutated transporters. The K134S and E122A mutants resembled the metal ion specificity of DCT1 (Table 1). Fig. 2 shows the uptake activity of DCT1, D124A, and the double mutant D124A/

Table 1. Uptake of different metal ions and complementation of SMF1 null mutants by DCT1 and mutants of loop I

Mutant	Fe uptake	Mn uptake	Co uptake	Complementation
DCT1	18.0 ± 1.8	45.4 ± 11.1	66.2 ± 7.3	+
G119A	<0.2	0	0	−
G119C	0			
G119V	0			
E122A	7.3 ± 2.2	9 ± 0.8	16.4 ± 4.5	−
D124A	3.8 ± 0.3	0.7 ± 0.1	1.7 ± 0.3	−
Q126D	<0.1	0	0	−
D124A + Q126D	3.26 ± 0	0.6 ± 0.2	2.2 ± 0.1	−
G119A + D124A + Q126D	0	0	0	−
K134S	2.3 ± 0.3	5.41 ± 0.5	9.3 ± 0.7	+

Representative experiments of oocytes obtained from at least three different frogs are shown. The results and standard deviations are expressed as metal uptake of pmol per oocyte per h. The yeast complementation assay was performed with *smf1*Δ mutant as described in *Materials and Methods.*

BIOCHEMISTRY

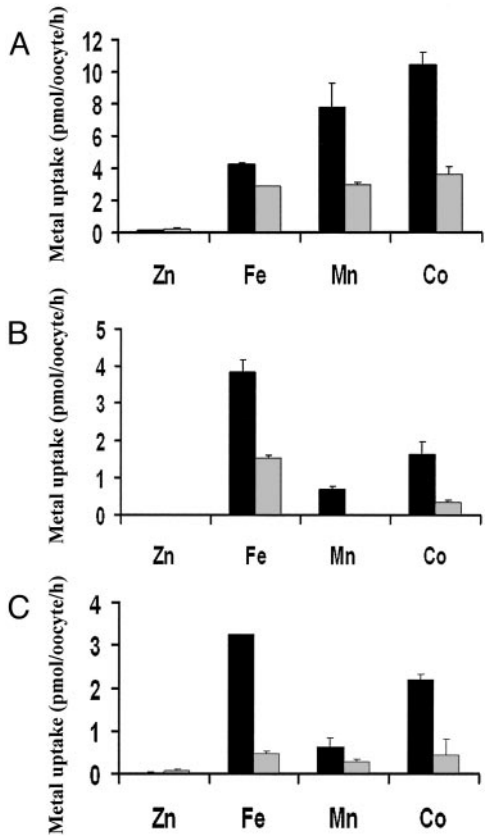

Fig. 2. Uptake of metal ions into *X. laevis* oocytes expressing DCT1, D124A mutant, and D124A/Q126D mutant. The uptake experiment was performed as described in *Materials and Methods*. (*A*) Metal ions uptake into DCT1-expressing oocytes. (*B*) Metal ions uptake into oocytes expressing the mutant D124A. (*C*) Metal ions uptake into oocytes expressing the double mutant D124A/Q126D. The uptake solution contained 100 mM NaCl, 2 mM KCl, 1 mM $MgCl_2$, 1 mM $CaCl_2$, 10 mM Hepes, 2 mM Mes, 2 mM ascorbic acid, and 7 μM of the indicated metal ion in its chloride form. The data for each bar represent means (after subtraction of the control values) + SEM (n = 15).

Q126D at pH 5.5 and 6.5. D124A exhibited appreciable Fe^{+2} uptake activity but very little Mn^{+2} uptake activity at pH 5.5, which was nullified when measured at pH 6.5 (Fig. 2*B*). The mutation Q126D abolished the uptake activity of the transporter (data not shown). However, elimination of a negatively charged residue two amino acids preceding it (D124A/Q126D) restored the activity of Fe^{+2} uptake and retained the relatively small Mn^{+2} uptake activity that was observed with the D124A mutant (Fig. 2*C*). These results indicate the importance of the D124 residue in the metal ion specificity of DCT1.

The sensitivity of the transporter to amino acid substitutions in this region is manifested best by the mutation of the conserved glycine at position 119 (Fig. 3). By PCR mistake, the triple mutant G119A/D124A/Q126D was obtained; it had no apparent transport activity but exhibited large pre-steady-state currents when expressed in *Xenopus* oocytes (see below and Figs. 4*B* and 5). The mutation G119A was created to serve as a control. The conservative substitution of G to A in this position resulted in almost complete inhibition of the metal ion uptake activity of the transporter (Table 1). Two additional mutations at this position (G119C and G119V) had the same phenotype; hence, the loss of glycine at this site and not the substitution of alanine was the reason for lack of activity.

Pre-Steady-State Currents of DCT1 Mutants and Their Proton-Binding Affinities. Pre-steady-state currents are excellent indicators for the expression level of electrogenic transporters in *Xenopus*

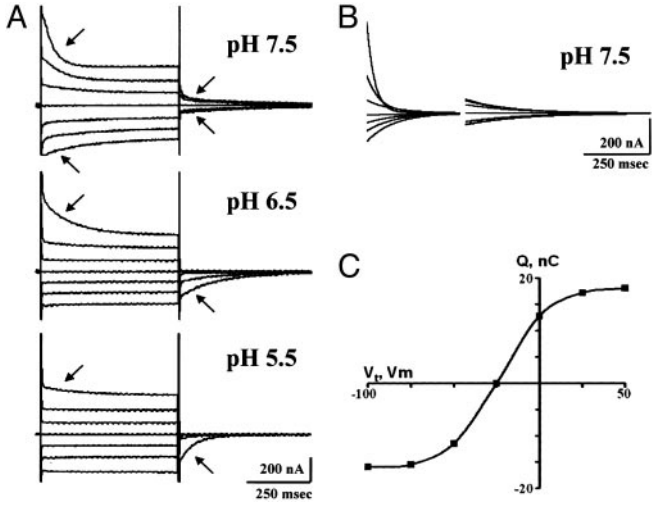

Fig. 3. The effect of pH on the pre-steady-state currents in the G119A mutant. The mutant was expressed in *X. laevis* oocytes, and the currents were recorded in a similar solution as described for Fig. 2 except that ascorbic acid and substrates were omitted. (*A*) Membrane current records at different pH values. The membrane voltage was transiently (500 msec) jumped to different imposed potentials, and the corresponding currents were recorded. The membrane potential was held at −25 mV and then jumped to varying potentials from +50 mV to −125 mV with 25-mV intervals. The transient currents are plotted against time, and the arrows indicate the pre-steady-state currents. Control oocytes do not exhibit pre-steady-state transient current. (*B*) Pre-steady-state charge movements were obtained from the total currents shown in *A* at pH 7.5 by subtraction of the capacitive and steady-state currents by using the fitted method (see *Materials and Methods*). (*C*) At each applied voltage, time integration of the off transients shown in *B* yielded the charge moved. The charge–voltage relationship obtained was fitted to a single Boltzmann function (see *Materials and Methods*). For the record shown, the Boltzmann parameters obtained from the fit were: Q_{max}, 34 nC; $V_{0.5}$, −23 mV.

oocytes (16). Therefore, the presence of pre-steady-state current in oocytes injected with mRNA-encoding mutated transporters that have little or no transport activity is a strong indication for their expression on the plasma membrane of the oocyte. The

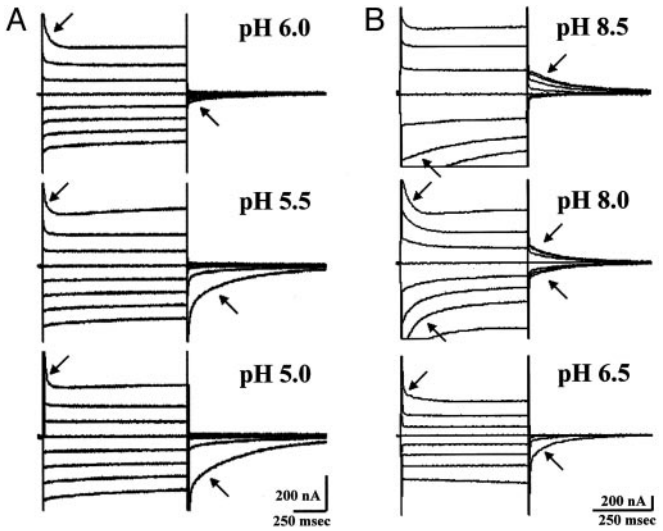

Fig. 4. The effect of the pH on the pre-steady-state currents of the double mutant D124A/Q126D and the triple mutant G119A/D124A/Q126D. (*A*) Double mutant D124A/Q126D. (*B*) Triple mutant G119A/D124A/Q126D. The experimental conditions were as described for Fig. 3 except that in *A* the membrane voltage was transiently jumped for 1 sec.

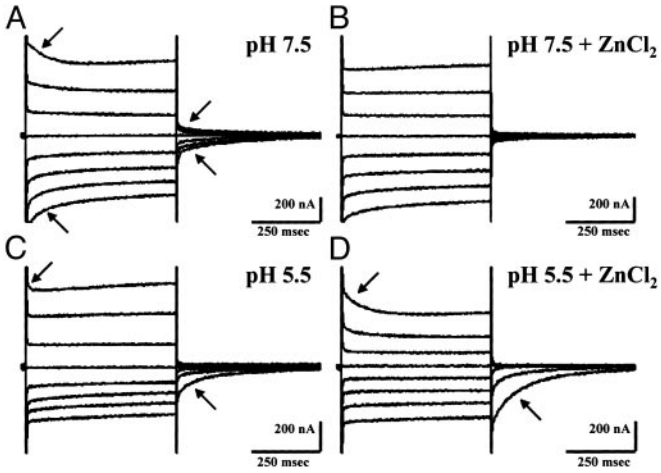

Fig. 5. Effect of Zn^{2+} on the pre-steady-state currents on the G119A/D124A/Q126D mutant at different pH values. The experiment was performed as described for Fig. 3 with pH of 7.5 and 5.5 in the presence or absence of 1 mM $ZnCl_2$.

mutation G119A in DCT1 had very little or no activity in the uptake of various divalent metal ions (Table 1). However, with no exception (seven independent mRNA injections) appreciable pre-steady-state currents were recorded (Fig. 3). In contrast to native DCT1, where the pre-steady-state currents appeared mainly at positively imposed potentials and their magnitude was optimal at pH 5.5 (10), those of G119A were optimal at pH 6.5–7.0 and appeared at all imposed potentials at pH 7.5 (Fig. 3*A*). This suggests that the conservative mutation G119A abolished not only the uptake activity, without affecting the assembly of the transporter, but also increased the affinity of the proton-binding site from ≈10 to 1 μM. This value was deduced qualitatively from the symmetry of the pre-steady-state currents in the various imposed potentials. A similar phenomenon was observed concerning the effect of Na^+ concentrations in the medium on the pre-steady state of $Na^+/Cl^-/\gamma$-aminobutyric acid transporters (22). To characterize further the features of the G119A mutant, we subtracted the capacitive and steady-state currents to yield the transient current shown in Fig. 3*B*. From the off transients, the time integration yielded the charge moved (Q), which was plotted as a function of imposed potentials (Fig. 3*C*). The data were fitted to the Boltzmann equation and at pH 7.5 Q_{max} of 34 nC and $V_{0.5}$ of −23 mV were determined. According to the Q_{max}, $\approx 2 \times 10^{11}$ transporters were expressed on the plasma membrane of each oocyte injected with the G119A mutant cRNA. Similar pre-steady-state currents, albeit somewhat smaller, were also recorded with the mutations G119C and G119V (data not shown). The measured $V_{0.5}$ at pH 6.5 of the native DCT1, the G119A, and the G119A/D124A/Q126D were −18, +18, and +27 mV, respectively. In all of the three transporters a 10-fold increase in proton concentration (one pH unit lower) shifted the $V_{0.5}$ by ≈40 mV. The time constant τ of the pre-steady-state current decay in G119A, in the potential jump from −25 to +50 mV, was ≈90 msec for the on response and ≈160 msec for the off response at pH 6.5. This is about double in comparison with DCT1 in the same conditions (Fig. 3).

Oocytes injected with the DCT1 mutant D124A showed pre-steady-state currents that were similar to those of the mutant G119A except that they had smaller magnitude (data not shown). Therefore, pre-steady-state currents in the double mutant D124A/Q126D were unexpected. As shown in Fig. 4*A*, the magnitude of the pre-steady-state currents was very high (Q_{max} = 180 nC at pH 5), indicating very high expression of the double mutant. At pH 5 in the potential jump from −25 to +50 mV, the on response was very fast ($\tau \approx 10$ msec) in comparison to the off response ($\tau \approx 400$ msec). The on rate increased with the elevation of external proton concentration (lower pH), and the off rate increased at higher external pH (Fig. 4*A*). This suggests that the double mutant altered the pK for proton binding toward lower affinity for protons in comparison with native DCT1. The pre-steady-state currents were visible only at low external pH values (practically disappeared at pH 6.0), their Q increasing by lowering the external pH, and this effect was not saturated even at pH 5.0. Although in Fig. 4*A* it is not apparent that the Q values of the on and off responses were equal, when we recorded on a time scale of 200 instead of 1,000 msec, the calculated Q values were equivalent (data not shown). In accordance with the sensitivity of the pre-steady-state currents to a moderate increase in the external pH, the metal ion uptake was also quite sensitive to higher pH values, and at pH 6.5 very little uptake activity was recorded (Fig. 2*C*). These observations suggest that proton binding in this mutant is a rate-limiting step in the uptake of the metal ions. However, the metal ion specificity mainly reflected the mutant in amino acid residue at position 124, namely the specificity of the double mutant D124A/Q126D resembled that of the D124A mutation (Fig. 2 *B* and *C*).

During the generation of the double mutant, a triple mutation G119A/D124A/Q126D was identified. This mutation is inactive in metal ion uptake but exhibited very high pre-steady-state currents with unique properties (Fig. 4*B*). In contrast to the double mutant D124A/Q126D, at low external pH very little or no pre-steady-state currents could be detected in the triple mutant. Starting with pH 6.5, appreciable pre-steady-state currents at positively imposed potentials could be observed, and the currents increased with increasing pH values. At pH 8 the currents were symmetrical and appeared in all imposed potentials, and at pH 8.5 the pre-steady-state currents were predominant at negatively imposed potentials. A plot of $V_{0.5}$ versus pH showed that the affinity for protons of the triple mutant shifted to pH 7.3 in comparison with 6.1 for DCT1 (9). This calculation is in line with the notion that the pK of the driving force in ion motive transporters corresponds to the ion concentration value right below the concentration in which symmetric pre-steady-state currents are obtained (22).

The addition of Co^{2+}, Mn^{2+}, or Fe^{2+} reduced the magnitude of the pre-steady-state currents in the triple mutant but did not abolish them (data not shown). It therefore was unexpected to discover that Zn^{2+} has an opposite effect on the pre-steady-state at different pH conditions in the medium. At pH 7.5, Zn^{2+} abolished the pre-steady-state currents (Fig. 5 *A* and *B*), but at pH 5.5, Zn^{2+} induced large pre-steady-state currents primarily at the positively induced potentials (Fig. 5 *C* and *D*). The calculated Q_{max} = 26 nC and $V_{0.5}$ = 26 mV were obtained for the native DCT1, and the same values were calculated for the triple mutant in the presence of Zn^{2+} at pH 5.5, which suggests that Zn^{2+} can bind to the triple mutants and its binding at low pH provides an environment for proton binding similar to that of the native DCT1. Moreover, the addition of Co^{2+} or Mn^{2+} at the same concentrations to the triple mutant failed to abolish the Zn^{2+}-induced pre-steady-state current, suggesting that the affinity of the triple mutant to Zn^{2+} is greater than to the other metal ions.

Metal Ion-Induced Steady-State Currents in DCT1 Mutants. At pH 5.5 and a millisecond time scale, oocytes injected with DCT1 cRNA exhibited pre-steady-state currents mainly at positively imposed potentials (9, 10). The addition of Mn^{2+} or Fe^{2+} resulted in disappearance of the pre-steady-state currents and appearance of large steady-state currents, especially at the negatively imposed potentials. At imposed potential of −125 mV, Zn^{2+} yielded significantly smaller currents. Fig. 6 shows the currents generated at different imposed potentials on DCT1 and its mutants by the addition of 1 mM $MnCl_2$ or $ZnCl_2$. As reported

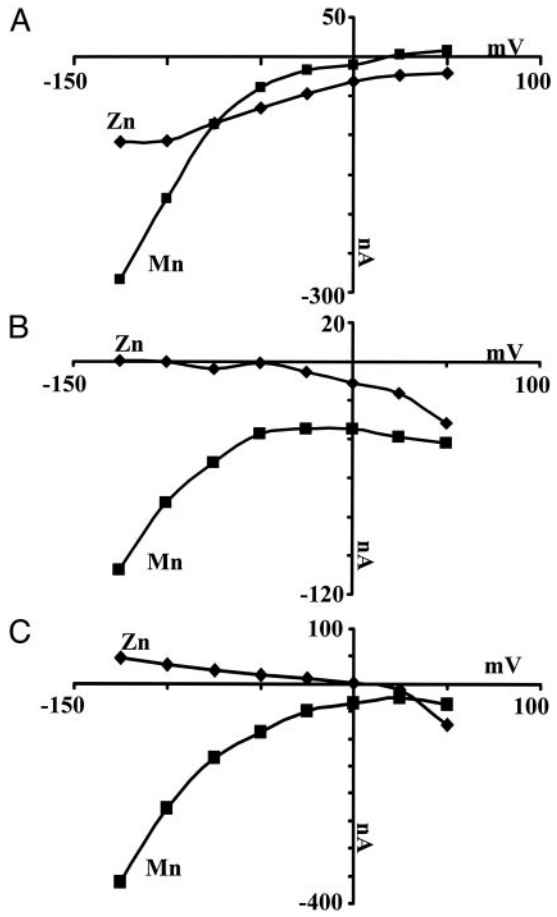

Fig. 6. Effect of imposed potential on manganese- and zinc-induced currents. The oocytes were incubated in medium containing 100 mM Mes (pH 5.5) in the presence or absence of 1 mM $MnCl_2$ or $ZnCl_2$. The oocyte membrane was held at −25 mV and stepped to a series of test voltages from +50 mV to −125 mV in steps of 25 mV. The differential currents in the presence and absence of the metal were recorded. (*A*) DCT1. (*B*) D124A mutant. (*C*) D124A + Q126D mutant. Diamonds, $\pm ZnCl_2$; squares, $\pm MnCl_2$.

previously, the addition of Zn^{2+} to DCT1-expressing oocytes generated large steady-state currents, especially at moderate negatively imposed potentials that were larger than those of Mn^{2+} (1). At −75 mV, the currents in the presence of both metals were equal. However, at −100 and −125 mV the currents generated by Mn^{2+} were much larger than those induced by Zn^{2+} (Fig. 6*A*). The mutation D124A, which had a relatively small Mn^{2+} uptake activity (Fig. 2*B* and Table 1), gave a large steady-state current in the presence of this cation (Fig. 6*B*). The mutation Q126D exhibited a negligible uptake activity and no metal ion-dependent steady-state currents (data not shown). However, the double mutant Q126D/D124A provided significant uptake activity (Fig. 2*C* and Table 1), maintained the metal ion specificity of D124A (Fig. 2 *B* and *C*), and exhibited large pre-steady-state currents (Fig. 4*C*). In contrast to its poor Mn^{2+} uptake activity, the addition of Mn^{2+} resulted in large steady-state currents, which reflect the proton slip through the mutated transporter (10, 23). With the mutant D124A and double mutant D124A/Q126D, Zn^{2+} failed to generate any significant current regardless of the potential. The small current at +50 mV is similar to the noninjected oocytes. In contrast, Mn^{2+} generated large steady-state currents in both mutants, and the effect of the potential was similar to that observed with native DCT1. The triple DCT1 mutant G119A/D124A/Q126D gave no significant steady-state currents in the presence of metal ions, as was the case with the G119A mutant. This suggests that the G119A substitution not only blocked the metal ion translocation but also eliminated the metal ion-induced proton slip.

Discussion

DCT1 and Smf1p are homologous metal ion transporters in mammals and yeast, respectively. In both DCT1 and Smf1p transporters, protons are the driving force for metal ion uptake, and in certain conditions both show an uncoupled current we called "slip" (9, 10, 23). DCT1 fully complements the null mutation of *SMF1* in yeast. Although the heterologous expression of DCT1 in yeast cells provided the opportunity to obtain suppressor mutants, its expression in *Xenopus* oocytes paved the way for the study of partial reactions by electrophysiology.

The coupling of metal ion transport to the proton electrochemical gradient presents several mechanistic problems. It is unusual that cationic driving force (protons) drives a cotransport of positively charged ions. The involvement of chloride in metal ion transport is not clear, and the mechanism of uncoupled proton current (slip) is not well characterized (23). At neutral pH, approximately one H^+ is translocated across the oocyte membrane by DCT1 per one Fe^{2+} ion (9). Under high proton concentration (low pH) the stoichiometry between H^+ and Fe^{2+} uptake increased from 1 to 10 (9, 10). Moreover, at low pH, changes in the membrane potential from +10 to −80 mV increased the charge/uptake ratio from 3 to ≈18 (9). The recorded steady-state current, however, seems to be indifferent to the nature of the metal ion. At pH 5.5 and at −50 mV, the addition of Co^{2+}, Mn^{2+}, Zn^{2+}, or Fe^{2+} generated similar currents of ≈100 nA (1, 10). However, uptake of labeled metal ions under similar conditions varied from >100 pmol per oocyte per h for Mn^{2+} and Co^{2+} and ≈50 pmol per oocyte per h for Fe^{2+} to no uptake of radiolabeled Zn^{2+}, yet Zn^{2+} generated currents that were as high as the other metal ions (10). Therefore, it is clear that two variable components contribute to the measured current: the protons and the metal ions that cross the membrane. Namely, the expressed transporter enables different quantities of proton slippage that takes place in the presence of metal ions, regardless of whether the particular metal ion is transported across the membrane. Under certain conditions, the proton current dominates the recorded charge movements across the membrane.

Recently it became apparent that protein segments predicted to reside outside the membranes play an important role in the transport process of several transporters (24, 25). We decided to substitute the amino acids in the predicted first outer loop of DCT1 that varied in comparison to Smf1p and mutate it according to the corresponding sequence in Smf1p. The mutants with the reciprocal substitutions of amino acids were analyzed for metal ion uptake activity and electrophysiology of *Xenopus* oocytes expressing these transporters. Their ability to complement the relevant yeast null mutant was the most demanding test, because it also required, in addition to proper biogenesis and assembly into the plasma membrane, substantial activity in manganese transport. When comparing the first loops of both transporters, it seems that some nonconservative substitutions of amino acids took place in the evolution of these transporters, during which time charged amino acids were either added or lost. Just like the recent alanine screening for charged amino acids in the transmembrane segments of DCT1 (26), here too not all the charged residues were crucial for the transporter's activity, but none exhibited the full activity of the original DCT1 in all of the measured parameters. However, in partial reactions, some mutants surprisingly outperformed the original transporter. Despite our approach, the most interesting results were obtained from a triple mutant (G119A/D124A/Q126D) in which, by serendipity,

a highly conserved glycine at position 119 was substituted by alanine.

One assumes that the interplay of pH, imposed membrane potential, and nature of the metal ion in the medium affect the steady-state recorded currents in oocytes expressing the DCT1 and its mutants. At pH 5.5, DCT1 exclusively exhibits pre-steady-state currents at positively imposed potential, and at pH 6.5 a symmetrical shape of pre-steady-state currents at positively and negatively imposed potentials is obtained. The symmetrical shape of the pre-steady state appeared close to the pH that was found to be the measured K_m of the DCT1 for proton binding (9). This phenomenon is similar to the γ-aminobutyric acid transporters expressed in *Xenopus* oocytes that show symmetrical pre-steady-state currents at Na^+ concentrations close to the K_m for the Na^+-driven transport (22, 27). Determination $V_{0.5}$ of DCT1 and some of the mutants in this work provided additional credence to the above notion. Thus we may conclude that the triple mutant G119A/D124A/Q126D exhibits high affinity for protons with a K_m of $\approx$50 nM, because the symmetrical appearance of the pre-steady state is at pH 8 (Fig. 4*B*). However, the double mutant D124A/Q126D had a lower affinity for protons even in comparison with DCT1. The proton-binding site did not saturate even at pH 5 (Fig. 4*A*). Thus, a single substitution of glycine residue to alanine resulted in an affinity change of $>$2 orders of magnitude. This glycine (G119), which is conserved in all of the family members, seems to be situated in a crucial position in the transporter. We propose that the external loop I in DCT1, and probably in the other family members, participates both in the proton and metal ion binding.

The effect of Zn^{2+} on the pre-steady-state currents in the triple mutant G119A/D124A/Q126D is noteworthy. Not only was Zn^{2+} the most effective metal ion in the dissipation of the pre-steady-state currents at pH 7.5 (Fig. 5*B*) but also, more unusually, induced large pre-steady-state currents at pH 5.5 (Fig. 5*D*). The dissipation at pH 7.5 could be explained by either Zn^{2+}-induced steady-state currents or substantial reduction of the Zn^{2+}-bound transporter's affinity to protons. We were not able to detect any Zn^{2+} transport or Zn^{2+}-induced steady-state currents; therefore, the latter explanation is more plausible. This may also explain the Zn^{2+}-induced pre-steady-state currents observed at low pH. Zn^{2+} binding to the triple mutant might change its conformation and restore the environment of the proton-binding site to its original state of the native DCT1, which enables large pre-steady-state currents at pH 5.5 and negligible ones at pH 7.5. However, the G119A substitution in the triple mutant prevents its transport ability and the metal-induced steady-state currents. The triple mutant G119A/D124A/Q126D exhibits very low affinity to the metal ions such as Co^{2+}, Mn^{2+}, and Fe^{2+}, which are the natural substrates of DCT1. This was manifested by the relatively small effect of these metal ions on abolishment of the pre-steady-state currents at pH 7.5 and lack of competition with the Zn^{2+}-induced pre-steady-state currents at pH 5.5 (data not shown).

Another finding of single and double amino acid substitutions in loop I is their involvement in the metal ion-induced proton slip. It was reported that in DCT1, at a holding potential of -50 mV, the Zn^{2+}-induced currents were larger than those of Mn^{2+}, Fe^{2+}, and Co^{2+} (10). In contrast, recorded metal ion-dependent steady-state currents at -125 mV were much smaller with Zn^{2+} than those induced by the other metal ions (Fig. 6). Although in DCT1 at pH 5.5 and negatively imposed potentials Zn^{2+} induced substantial steady-state currents, in the D124A and the double mutant D124A/Q126D Zn^{2+} failed to induce any significant steady-state currents, yet Mn^{2+} induced as large a steady-state current as in DCT1 (Fig. 6). This may be due to a complete loss of Zn^{2+}-binding ability in these mutants or uncoupling of the Zn^{2+} binding from the proton translocation pathway. Inhibition by Zn^{2+} of Fe^{2+} uptake by these mutants (data not shown) eliminates the first possibility. Therefore, this region in the DCT1 must also be involved in the coupling mechanism between the metal ion and the translocation that generates the steady-state current.

This project was funded by European Union Grant QLRT-2001-00533 EFFEXPORT.

1. Nelson, N. (1999) *EMBO J.* **18,** 4361–4371.
2. Forbes, J. R. & Gros, P. (2001) *Trends Microbiol.* **9,** 397–403.
3. Van Ho, A., Ward, D. M. & Kaplan, J. (2002) *Annu. Rev. Microbiol.* **56,** 237–261.
4. Goswami, T., Rolfs, A. & Hediger, M. A. (2002) *Biochem. Cell Biol.* **80,** 679–689.
5. Supek, F., Supekova, L., Nelson, H. & Nelson, N. (1996) *Proc. Natl. Acad. Sci. USA* **93,** 5105–5110.
6. Supek, F., Supekova, L., Nelson, H. & Nelson, N. (1997) *J. Exp. Biol.* **200,** 321–330.
7. Liu, X. F., Supek, F., Nelson, N. & Culotta, V. C. (1997) *J. Biol. Chem.* **272,** 11763–11769.
8. Chen, X.-Z., Peng, J.-B., Cohen, A., Nelson, H., Nelson, N. & Hediger, M. A. (1999) *J. Biol. Chem.* **274,** 35089–35094.
9. Gunshin, H., Mackenzie, B., Berger, U. V., Gunshin, Y., Romero, M. F., Boron, W. F., Nussberger, S., Gollan, J. L. & Hediger, M. A. (1997) *Nature* **388,** 482–488.
10. Sacher, A., Cohen, A. & Nelson, N. (2001) *J. Exp. Biol.* **204,** 1053–1061.
11. Liu, X. F. & Culotta, V. C. (1999) *J. Mol. Biol.* **289,** 885–891.
12. Pinner, E., Gruenheid, S., Raymond, M. & Gros, P. (1997) *J. Biol. Chem.* **272,** 28933–28938.
13. Su, M. A., Trenor, C. C., Fleming, J. C., Fleming, M. D. & Andrews, N. C. (1998) *Blood* **92,** 2157–2163.
14. Cohen, A., Nelson, H. & Nelson, N. (2000) *J. Biol. Chem.* **275,** 33388–33394.
15. Noumi, T., Beltrán, C., Nelson, H. & Nelson, N. (1991) *Proc. Natl. Acad. Sci. USA* **88,** 1938–1942.
16. Wright, E. M., Loo, D. D., Panayotova-Heiermann, M., Lostao, M. P., Hirayama, B. H., Mackenzie, B., Boorer, K. & Zampighi, G. (1994) *J. Exp. Biol.* **196,** 197–212.
17. Nelson, H. & Nelson, N. (1990) *Proc. Natl. Acad. Sci. USA* **87,** 3503–3507.
18. Loo, D. D., Hazama, A., Supplisson, S., Turk, E. & Wright, E. M. (1993) *Proc. Natl. Acad. Sci. USA* **90,** 5767–5771.
19. Loo, D. D., Hirayama, B. A., Gallardo, E. M., Lam, J. T., Turk, E. & Wright, E. M. (1998) *Proc. Natl. Acad. Sci. USA* **95,** 7789–7794.
20. Chen, X.-Z., Shayakul, C., Berger, U. V., Tian, W. & Hediger, M. A. (1998) *J. Biol. Chem.* **273,** 20972–20981.
21. Grossman, T. R. & Nelson, N. (2002) *FEBS Lett.* **527,** 125–132.
22. Nussberger, S., Steel, A., Trotti, D., Romero, M. F., Boron, W. F. & Hediger, M. A. (1997) *J. Biol. Chem.* **272,** 7777–7785.
23. Nelson, N., Sacher, A. & Nelson, H. (2002) *Nat. Rev. Mol. Cell Biol.* **3,** 876–881.
24. Tamura, S., Nelson, H., Tamura, A. & Nelson, N. (1995) *J. Biol. Chem.* **270,** 28712–28715.
25. Kwaw, I., Sun, J. & Kaback, H. R. (2000) *Biochemistry* **39,** 3134–3140.
26. Lam-Yuk-Tseung, S., Govoni, G., Forbes, J. & Gros, P. (2003) *Blood* **101,** 3699–3707.
27. Grossman, T. R. & Nelson, N. (2003) *Neurochem. Int.* **43,** 431–443.